Available online at www.sciencedirect.com
SCIENCE DIRECT®
Bioorganic & Medicinal Chemistry Letters
ELSEVIER
Bioorganic & Medicinal Chemistry Letters 14 (2004) 1247–1251

Synthesis, biodistribution and micro-PET imaging of radiolabeled antimitotic agent T138067 analogues

Xiangshu Fei,[a] Qi-Huang Zheng,[a,*] Ji-Quan Wang,[a] K. Lee Stone,[a] Tanya D. Martinez,[a] Kathy D. Miller,[b] George W. Sledge[b] and Gary D. Hutchins[a]

[a]*Department of Radiology, Indiana University School of Medicine, Indianapolis, IN 46202, USA*
[b]*Department of Medicine, Indiana University School of Medicine, Indianapolis, IN 46202, USA*

Received 29 May 2003; accepted 10 December 2003

Abstract—Radiolabeled antimitotic agents [^{11}C]T138067 and [^{18}F]T138067 have been synthesized for evaluation as new potential positron emission tomography (PET) biomarkers for cancer imaging. In vivo biodistribution and micro-PET imaging of [^{11}C]T138067 were performed in breast cancer animal models MCF-7 transfected with IL-1α implanted athymic mice and MDA-MB-435 implanted athymic mice. The results suggest that the uptakes of [^{11}C]T138067 in both MCF-7 transfected with IL-1α tumor and MDA-MB-435 tumor are non-specific binding.

Antimitotic drugs have emerged as an effective treatment for a variety of cancers.[1] The new antimitotic agent T138067 is an irreversible inhibitor of tubulin polymerization, which is currently in phase II clinical trials and is effective against many tumor types, including those that express the multidrug resistant (MDR) phenotype.[2–5] The anticancer mechanism of T138067 is that it has been shown to covalently bind to cysteine-239 on β-tubulin isoforms 1, 2, and 4 by the way of a nucleophilic aromatic substitution reaction, and the covalent modification of β-tubulin inhibits the polymerization of the α,β-tubulin heterodimers into microtubules, which leads to cell arrest at the G2/M cell cycle boundary followed by apoptosis.[2]

In order to develop novel cancer biomarkers for molecular imaging,[6] a series of positron emission tomography (PET) cancer imaging agents that target either receptors or enzymes have been synthesized in this laboratory.[7–15] Tubulin polymerization provides a target for the in vivo biomedical imaging technique PET to image cancers. Radiolabeled antimitotic agent T138067 analogues labeled with positron emitting radionuclides carbon-11 or fluorine-18 may enable non-invasive monitoring of cancer tubulin polymerization and its response to antimitotic drug treatment using PET. Here we report the synthesis of [^{11}C]T138067 and [^{18}F]T138067, and the in vivo biodistribution and micro-PET imaging of [^{11}C]T138067.

The synthesis of [^{11}C]T138067 and [^{18}F]T138067 is shown in Scheme 1.

The reaction of two commercially available starting materials pentafluorobenzenesulfonyl chloride (**2**) and 3-fluoro-4-methoxyaniline (**3**) in methanol provided target compound *N*-(3-fluoro-4-methoxy-phenyl)-2,3,4,5,6-pentafluorobenzenesulfonamide (T138067, **1**) in 85% chemical yield. The demethylation of **1** with BBr_3 in methylene chloride gave the phenol precursor *N*-(3-fluoro-4-hydroxy-phenyl)-2,3,4,5,6-pentafluorobenzenesulfonamide (**4**) in 43% chemical yield for carbon-11 radiolabeling. The phenol precursor **4** was alkylated with [^{11}C]methyl triflate[16,17] under basic conditions using tetrabutylammonium hydroxide (TBAH) through ^{11}C-*O*-methylation method and isolated by solid-phase extraction (SPE) purification[9,18–20] to produce pure target tracer [^{11}C]T138067 ([^{11}C]**1**) in 45–60% radiochemical yields based on $^{11}CO_2$, decay corrected to end of bombardment (EOB), in 20–25 min synthesis time. The large polarity difference between the phenol precursor and the labeled O-methylated product permitted the use of SPE technique for purification of radiotracer from radiolabeling reaction mixture. The reaction

* Corresponding author. Tel.: +1-317-278-4671; fax: +1-317-278-9711; e-mail: qzheng@iupui.edu

0960-894X/$ - see front matter © 2003 Elsevier Ltd. All rights reserved.
doi:10.1016/j.bmcl.2003.12.061

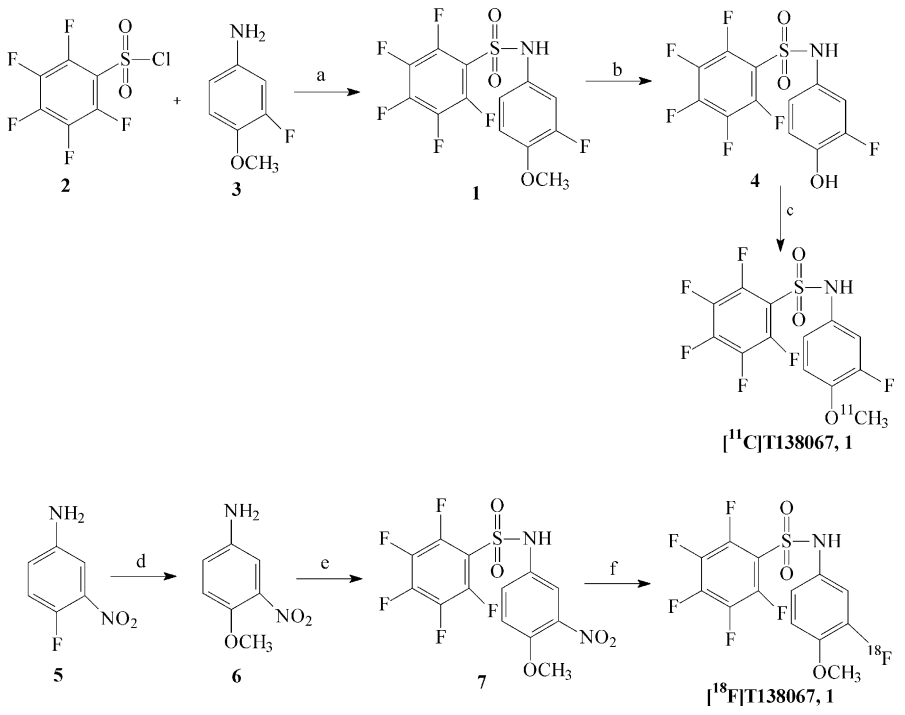

Scheme 1. Synthesis of [^{11}C]T138067 and [^{18}F]T138067: (a) MeOH; (b) BBr_3, CH_2Cl_2; (c) $^{11}CH_3OTf$, TBAH, CH_3CN; (d) NaOMe/MeOH; (e) **2**, MeOH; (f) $K^{18}F$, $K_{2.2.2}$, CH_3CN.

mixture was diluted with $NaHCO_3$ (0.1 M) and loaded onto C-18 cartridge by gas pressure. The cartridge column was washed with water to remove unreacted phenol precursor, non-reacted [^{11}C]methyl triflate and reaction solvent acetonitrile, and then final labeled product was eluted with ethanol. Chemical purity, radiochemical purity, and specific radioactivity were determined by analytical HPLC methods, which employed a Prodigy (Phenomenex) 5 μm C-18 column, 4.6×250 mm; 3:1:3 CH_3CN: MeOH: 20 mM, pH 6.7 $KHPO_4^-$ mobile phase, 1.5 mL/min flow rate, UV (240 nm) and γ-ray (NaI) flow detectors. Retention times in this HPLC system were: RT**4** = 2.17 min, RT[^{11}C]**1** = 5.30 min. The chemical purity of precursor **4** and standard sample **1** was >95%, radiochemical purity of target radiotracers [^{11}C]**1** was >99%, and the chemical purity of target radiotracer [^{11}C]**1** was >95%. The specific activity of target radiotracers [^{11}C]**1** was 0.6–0.8 Ci/μmol (n = 3–5) at end-of-synthesis (EOS).

The commercially available starting material 4-fluoro-3-nitroaniline (**5**) was reacted with NaOMe/MeOH to convert to 4-methoxy-3-nitroaniline (**6**) in 93% chemical yield. The reaction of **2** with **6** in methanol provided the nitro-precursor *N*-(4-methoxy-3-nitro-phenyl)-2,3,4,5,6-pentafluorobenzenesulfonamide (**7**) in 82% chemical yield for fluorine-18 radiolabeling. The nitro-precursor **7** was labeled by a conventional nucleophilic substitution[14] with K[^{18}F]/Kryptofix 2.2.2 in CH_3CN at 120 °C for 20 min to provide target tracer [^{18}F]T138067 ([^{18}F]**1**). The radiolabeling reaction was monitored by analytical radio-HPLC method, in which we employed a HPLC system aforementioned. Retention times in the analytical HPLC system were: RT**7** = 3.23 min, RT[^{18}F]**1** = 5.48 min, RTK[^{18}F] = 1.88 min. The radiolabeling mixture was passed through a Silica Sep-Pak to remove Kryptofix 2.2.2 and non-reacted [^{18}F]fluoride. The large polarity difference between nitro-precursor, labeled product and Kryptofix 2.2.2, non-reacted [^{18}F]fluoride permitted the use of a simple SPE technique[21,22] for fast isolation of nitro-precursor and labeled product from the radiolabeling reaction mixture. The key part in this technique is a SiO_2 Sep-Pak type cartridge, which contains ~0.5–2 g of adsorbent. The Sep-Pak was eluted with MeOH and the solvent was evaporated under high vacuum to give the mixture residue of the precursor and product. The existence of the catalyst Kryptofix 2.2.2 and non-reacted [^{18}F]fluoride would affect the purification of labeled product from its mixture with precursor; therefore, they needed to be removed before [^{18}F]**1** was separated from the mixture. This mixture was purified with SPE method instead of HPLC method so that it will be amenable for automation. The residue was dissolved in $NaHCO_3$ (0.1 M, 1 mL), passed through a C-18 cartridge by gas pressure to remove precursor by simple SPE with water. The large polarity difference between precursor **7** and radiolabeled product [^{18}F]**1** permitted the use of SPE technique for fast purification of radiotracer [^{18}F]**1** from its mixture with **7**. The radiochemically pure compound [^{18}F]**1** was isolated with ethanol from the C-18 cartridge and evaporated to remove organic solvent and formulated with saline. The radiochemical yield of [^{18}F]**1** was 30–35%, and the synthesis time was 60–70 min from EOB. Chemical purity, radiochemical purity, and specific radioactivity were determined by analytical HPLC method. The chemical purities of precursor **7** and standard sample **1** were >95%, the radiochemical purity of target radiotracer [^{18}F]**1** was >99%, and the chemical purity of radiotracer [^{18}F]**1** was ~93%. The

specific radioactivities of radiotracer [^{18}F]**1** were 0.8–1.2 Ci/μmol ($n = 3$–5) at EOS.

Compounds **1**, **4** and **7** have analytical data such as mp, ^{1}H NMR and MS in agreement with the indicated structures.[23]

In vivo biodistribution studies of [^{11}C]T138067 were performed in breast cancer animal models MCF-7 transfected with IL-1α implanted athymic mice and MDA-MB-435 implanted athymic mice. Tumor-bearing athymic mice utilized were prepared as described in our previous work.[13] Athymic mice 8 weeks post-xenograft implantation were injected intravenously (iv) with sub-pharmacologic doses (1–3 mCi) of [^{11}C]T138067 via the tail vein while under conscious restraint. At 30 min post injection, mice were sacrificed by decapitation under halothane anesthesia, their tissues quickly excised, weighed, and the decay-corrected radioactive content measured using a Packard Cobra Quantum gamma counter. The tissue localization at the various time points, expressed as % of injected dose per gram of tissue (% id/g), weight normalized % id/g (kg% id/g) and % of injected dose per organ were calculated from the tissue count and weight data using an Excel spreadsheet program. In vivo biodistribution data of [^{11}C]T138067 in MCF-7 transfected with IL-1α implanted athymic mice and MDA-MB-435 implanted athymic mice are listed in Tables 1 and 2, which showed the uptakes of [^{11}C]T138067 in these tumors were 1.51±0.39% dose/g in MCF-7 transfected with IL-1α implanted mice, 1.92±0.08% dose/g in MDA-MB-435 implanted mice, respectively; the ratios of tumor/muscle (T/M) and tumor/blood (T/B) were 0.89±0.23 (T/M, MCF-7′s), 0.94±0.36 (T/B, MCF-7's); and 1.01±0.26 (T/M, MDA-MB-435), 5.63±0.71 (T/B, MDA-MB-435), respectively, at 30 min post iv injection. The data presented here represented the average value in three tumor mice. The tumor/muscle and the tumor/blood ratios are in a range of 0.9–5.6, and they are not very high. In comparison with blood, brain, heart, liver, lungs, spleen, kidneys, small intestine, bone and muscle, biodistribution studies of [^{11}C]T138067 in MCF-7 transfected with IL-1α implanted athymic mice and MDA-MB-435 implanted athymic mice did not show higher uptakes in tumors than in other organs. A considerable uptake was observed in liver, lungs, kidneys and small intestine. These results indicate that the uptakes of [^{11}C]T138067 in both MCF-7 transfected with IL-1α tumor and MDA-MB-435 tumor are most likely the result of non-specific binding.

Table 1. Biodistribution data of [^{11}C]T138067 in MCF-7 transfected with IL-1α implanted athymic mice at 30 min post iv injection. Values are mean±standard deviation (SD) of % id/g

Tissue	MCF-7 transfected with IL-1α tumor-bearing mice ($n = 3$)
Blood	1.68±0.30
Brain	1.53±0.10
Heart	1.75±0.08
Liver	6.79±0.98
Lungs	4.95±0.49
Spleen	2.01±0.17
Kidneys	3.34±0.37
Small intestine	5.16±1.78
Bone	1.31±0.60
Muscle	1.70±0.22
Tumor	1.51±0.39
Tumor/muscle (T/M) ratio	0.89±0.23
Tumor/blood (T/B) ratio	0.94±0.36

In vivo micro-PET imaging studies were performed in the Indy-PET II scanner developed by Hutchins et al.[24,25] The mouse was anesthetized with acepromazine (0.2 mg/kg, i.m.) and torbugesic (0.2 mg/kg, i.m.). 1 mCi of [^{11}C]T138067 was administered intravenously to the mouse via the tail vein. The micro-PET images of [^{11}C]T138067 in both breast cancer athymic mice were acquired in Indy-PET II scanner for 15 min static scans from a MCF-7 transfected with IL-1α tumor-bearing mouse or a MDA-MB-435 tumor-bearing mouse at 30

Table 2. Biodistribution data of [^{11}C]T138067 in MDA-MB-435 implanted athymic mice at 30 min post iv injection. Values are mean ±standard deviation (SD) of % id/g

Tissue	MDA-MB-435 tumor-bearing mice ($n = 3$)
Blood	0.35±0.06
Brain	1.03±0.09
Heart	8.54±2.79
Liver	14.92±3.21
Lungs	9.20±3.51
Spleen	2.95±0.33
Kidneys	17.62±3.60
Small intestine	6.19±1.18
Bone	1.75±0.66
Muscle	1.99±0.50
Tumor	1.92±0.08
Tumor/muscle (T/M) ratio	1.01±0.26
Tumor/blood (T/B) ratio	5.63±0.71

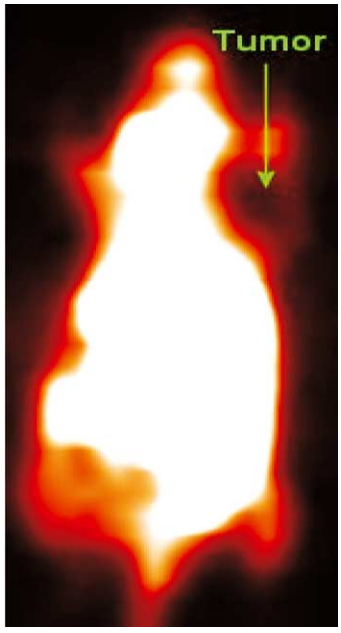

Figure 1. Micro-PET image of [^{11}C]T138067 in a MCF-7 transfected with IL-1α implanted athymic mouse.

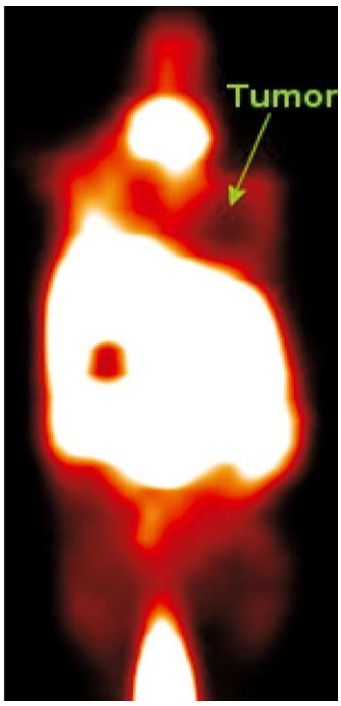

Figure 2. Micro-PET image of [^{11}C]T138067 in a MDA-MB-435 implanted athymic mouse.

min post iv injection of 1 mCi of the tracer. The images are shown in Figures 1 and 2. The tumor area in the tumor-bearing mouse was pointed out by the arrow in the Figures. Both MCF-7 transfected with IL-1α tumor and MDA-MB-435 tumor were not visible with the tracer [^{11}C]T138067 as clearly shown in the in vivo micro-PET images.

In summary, the synthetic procedures that provide radiolabeled antimitotic agents [^{11}C]T138067 and [^{18}F]T138067 have been developed. From the in vivo study results, we concluded that while in vitro experiments indicate efficacy of antimitotic drug T138067,[2] kinetic factors and rapid blood clearance[26] make [^{11}C]T138067 unsuitable as tracer for nuclear medicine imaging of tubulin polymerization. Based on the results of [^{11}C]T138067, we may suggest both [^{11}C]T138067 and [^{18}F]T138067 will not be suitable as PET cancer imaging agents. This type of work regards simply radiolabeling a drug that has been developed for therapeutic purposes as is the case with T138067 which is in phase II clinical trials indicates that successful drugs for therapeutic and imaging purposes almost invariably demonstrate different pharmacokinetic profiles to each other and by far the largest majority of useful imaging agents would not be useful in therapy.

Acknowledgements

This work was partially supported by the Susan G. Komen Breast Cancer Foundation grant IMG 02-1550 (to Q.H.Z.), the Indiana University American Cancer Society (ACS) Institutional Grant Committee grant IRG-84-002-17 (to Q.H.Z.), the Indiana University Cores Centers of Excellence in Molecular Hematology (CCEMH) pilot and feasibility (P/F) grant (to Q.H.Z.), the National Institutes of Health/National Cancer Institute grant P20CA86350 (to G.D.H.), the Indiana 21st Century Research and Technology Fund (to G.D.H.), and the Lilly Endowment Inc. to Indiana Genomics Initiative (INGEN) of Indiana University. We thank Dr. Bruce Mock, Barbara Glick-Wilson and Michael Sullivan for the efforts in producing carbon-11 precursors and [^{18}F]fluoride. The IL-1α transfected cells were a kind gift of Dr. Harikrishna Nakshatri. The referees' criticisms and editor's comments for the revision of the manuscript are greatly appreciated.

References and notes

1. Rowinsky, E. K.; Donehower, R. C. *Pharmacol. Ther.* **1991**, *52*, 35.
2. Shan, B.; Medina, J. C.; Santha, E.; Frankmoelle, W. P.; Chou, T.-C.; Learned, R. M.; Narbut, M. R.; Scott, D.; Wu, P.; Jaen, J. C.; Rosen, T.; Timmermans, P. B.; Beckmann, H. *Proc. Natl. Acad. Sci. U.S.A.* **1999**, *96*, 5686.
3. Medina, J. C.; Roche, D.; Shan, B.; Learned, R. M.; Frankmoelle, W. P.; Clark, D. L.; Rosen, T.; Jaen, J. C. *Bioorg. Med. Chem. Lett.* **1999**, *9*, 1843.
4. Medina, J. C.; Shan, B.; Beckmann, H.; Farrell, R. P.; Clark, D. L.; Learned, R. M.; Roche, D.; Li, A.; Baichwal, V.; Case, C.; Baeurle, P. A.; Rosen, T.; Jaen, J. C. *Bioorg. Med. Chem. Lett.* **1998**, *8*, 2653.
5. Rubenstein, S. M.; Baichwal, V.; Beckmann, H.; Clarl, D. L.; Frankmoelle, W.; Roche, D.; Santha, E.; Schwender, S.; Thoolen, M.; Ye, Q.; Jaen, J. C. *J. Med. Chem.* **2001**, *44*, 3599.
6. Weissleder, R.; Mahmood, U. *Radiology* **2001**, *219*, 316.
7. Fei, X.; Zheng, Q.-H.; Hutchins, G. D.; Liu, X.; Stone, K. L.; Carlson, K. A.; Mock, B. H.; Winkle, W. L.; Glick-Wilson, B. E.; Miller, K. D.; Fife, R. S.; Sledge, G. W.; Sun, H. B.; Carr, R. E. *J. Labelled Cpd. Radiopharm.* **2002**, *45*, 449.
8. Zheng, Q.-H.; Fei, X.; DeGrado, T. R.; Wang, J.-Q.; Stone, K. L.; Martinez, T. D.; Gay, D. J.; Baity, W. L.; Mock, B. H.; Glick-Wilson, B. E.; Sullivan, M. L.; Miller, K. D.; Sledge, G. W.; Hutchins, G. D. *Nucl. Med. Biol.* **2003**, *30*, 753.
9. Zheng, Q.-H.; Fei, X.; Liu, X.; Wang, J.-Q.; Sun, H. B.; Mock, B. H.; Stone, K. L.; Martinez, T. D.; Miller, K. D.; Sledge, G. W.; Hutchins, G. D. *Nucl. Med. Biol.* **2002**, *29*, 761.
10. Liu, X.; Zheng, Q.-H.; Fei, X.; Wang, J.-Q.; Ohannesian, D. W.; Erickson, L. C.; Stone, K. L.; Hutchins, G. D. *Bioorg. Med. Chem. Lett.* **2003**, *13*, 641.
11. Zheng, Q.-H.; Liu, X.; Fei, X.; Wang, J.-Q.; Ohannesian, D. W.; Erickson, L. C.; Stone, K. L.; Hutchins, G. D. *Nucl. Med. Biol.* **2003**, *30*, 405.
12. Zheng, Q.-H.; Liu, X.; Fei, X.; Wang, J.-Q.; Ohannesian, D. W.; Erickson, L. C.; Stone, K. L.; Martinez, T. D.; Miller, K. D.; Hutchins, G. D. *J. Labelled Cpd. Radiopharm.* **2002**, *45*, 1239.
13. Zheng, Q.-H.; Stone, K. L.; Mock, B. H.; Miller, K. D.; Fei, X.; Liu, X.; Wang, J.-Q.; Glick-Wilson, B. E.; Sledge, G. W.; Hutchins, G. D. *Nucl. Med. Biol.* **2002**, *29*, 803.
14. Wang, J.-Q.; Zheng, Q.-H.; Fei, X.; Mock, B. H.; Hutchins, G. D. *Bioorg. Med. Chem. Lett.* **2003**, *13*, 3933.
15. Zheng, Q.-H.; Wang, J.-Q.; Fei, X.; Hutchins, G. D. *Synthesis* **2003**, 2785.
16. Jewett, D. M. *Appl. Radiat. Isot.* **1992**, *43*, 1383.

17. Mock, B. H.; Mulholland, G. K.; Vavrek, M. T. *Nucl. Med. Biol*. **1999**, *26*, 467.
18. Zheng, Q.-H.; Mulholland, G. K. *Nucl. Med. Biol*. **1996**, *23*, 981.
19. Zheng, Q.-H.; Mulholland, G. K. *J. Labelled Cpd. Radiopharm*. **1997**, *40* (Suppl. 1), 551.
20. Zheng, Q.-H.; Winkle, W.; Carlson, K.; Mulholland, G. K. *J. Labelled Cpd. Radiopharm*. **1997**, *40* (Suppl. 1), 548.
21. Zheng, Q.-H.; Liu, X.; Fei, X.; Wang, J.-Q.; Mock, B. H.; Glick-Wilson, B. E.; Sullivan, M. L.; Hutchins, G. D. *Bioorg. Med. Chem. Lett*. **2003**, *13*, 1787.
22. Mulholland, K. M.; Zheng, Q.-H.; Mock, B. H.; Vavrek, M. T. *J. Labelled Cpd. Radiopharm*. **1999**, *42* (Suppl. 1), S459.
23. **1**, mp 114–115 °C. ^{1}H NMR (300 MHz, $CDCl_3$) δ 3.86 (s, 3H, OCH_3), 6.86–6.91 (t, $J = 8.8$ Hz, 1H, Ph-H), 6.91–6.92 (d, $J = 8.0$ Hz, 1H, Ph-H), 6.98–7.03 (dd, $J = 2.2$, 11.8 Hz, 1H, Ph-H). **4**, mp 115–116 °C. ^{1}H NMR (300 MHz, $CDCl_3$) δ 1.69 (s, 1H, OH), 5.27–5.28 (d, $J = 4.0$ Hz, 1H, NH), 6.82–6.82 (d, $J = 8.0$ Hz, 1H, Ph-H), 6.91–6.96 (t, $J = 8.0$ Hz, 1H, Ph-H), 7.04–7.09 (dd, $J = 2.4$, 11.0 Hz, 1H, Ph-H). LRMS (EI, CH_4, m/z): 358.0 ($M^+ + 1$, 12%), 126.0 (100%). HRMS (EI, CH_4, m/z): calcd For $C_{12}H_5F_6NO_3S$ 356.9894, found 356.9887. **7**, mp 94–95 °C. ^{1}H NMR (300 MHz, $CDCl_3$) δ 3.95 (s, 3H, OCH_3), 7.07–7.10 (d, $J = 9.5$ Hz, 1H, Ph-H), 7.52–7.55 (dd, $J = 2.2$, 8.8 Hz, 1H, Ph-H), 7.67–7.68 (d, $J = 3.0$ Hz, 1H, Ph-H).
24. Rouze, N. C.; Hutchins, G. D. *IEEE Trans. Nucl. Sci*. **2003**, *50*, 1491.
25. Frese, T.; Rouze, N. C.; Bouman, C. A.; Sauer, K.; Hutchins, G. D. *IEEE T. Med. Imaging* **2003**, *22*, 258.
26. Bonasera, T. A.; Ortu, G.; Rozen, Y.; Krais, R.; Freedman, N. M. T.; Chisin, R.; Gazit, A.; Levitzki, A.; Mishani, E. *Nucl. Med. Biol*. **2001**, *28*, 359.